Research Paper

Apoptosis Induction by Iron Radiation via Inhibition of Autophagy in *Trp53*⁺/⁻ Mouse Testes: Is Chronic Restraint-Induced Stress a Modifying Factor?

Hongyan Li[1, 2, 3#], Bing Wang[4#✉], Hong Zhang[1, 2, 3, 5✉], Takanori Katsube[4], Yi Xie[1, 2, 3], Lu Gan[1, 2, 3]

1. Department of Radiation Medicine, Institute of Modern Physics, Chinese Academy of Sciences, Lanzhou 730000, China
2. Key Laboratory of Heavy Ion Radiation Biology and Medicine of Chinese Academy of Sciences, Lanzhou 730000, China
3. Key Laboratory of Basic Research on Heavy Ion Radiation Application in Medicine, Lanzhou 730000, China
4. National Institute of Radiological Sciences, National Institutes for Quantum and Radiological Science and Technology, Chiba 263-8555, Japan
5. Gansu Wuwei Tumor Hospital, Department of Science and Technology, Wuwei 733000, China

#These authors contributed equally to this work.

✉ Corresponding authors: Department of Radiation Medicine, Institute of Modern Physics, Chinese Academy of Sciences, Lanzhou 730000, China. Tel: +96-931-4969344; fax: +86-931-8272100. *E-mail address:* zhangh@impcas.ac.cn. Department of Radiation Effects Research, National Institute of Radiological Sciences, National Institutes for Quantum and Radiological Science and Technology, Chiba 263-8555, Japan. Tel: +81-43-206-3093; fax: +81-43-251-4582. *E-mail address:* wang.bing@qst.go.jp.

Abstract

We used chronic restraint-induced stress (CRIS) and iron ionizing radiation (IR) to mimic human exposure to psychological stress (PS) and IR in a mouse model, and to investigate the relationship among endoplasmic reticulum stress (ERS), apoptosis and autophagy in testicular toxicity. Male *Trp53*⁺/⁻ C57BL/6N mice were restrained for 6 h/day for 28 consecutive days, and total body irradiation with 0.1 or 2 Gy iron ion beam was performed on the day 8. Histopathological observation showed severely damaged spermatogenic cells, increased apoptotic cells, caspase-3 activation and cytochrome c release, indicating that IR and CRIS+IR induced testicular cell apoptosis. Upregulation of GRP78 (78-kDa glucose-regulated protein) suggested that IR and CRIS+IR induced ERS in the testes, and further analysis showed that apoptosis was enhanced by ERS through activation of the PERK/eIF2α/ATF4/CHOP pathway. Decreased expression of LC3II, Atg5 (autophagy related 5) and Beclin 1, and increased expression of p62, combined with ultrastructural changes seen under transmission electron microscopy, suggest that IR and CRIS+IR inhibit autophagosome formation. This process was related to inhibition of autophagy via activation of the PI3K/AKT/mTOR pathway under ERS. We showed that apoptosis was strengthened and autophagy was inhibited by ERS in mouse testes induced by IR and CRIPS+IR. These results showed that CRIS+IR had no difference in apoptosis induction and autophagy inhibition compared with IR alone. CIRS alone could induce apoptosis only in Leydig cells and its induction of pathological and molecular changes in testicular tissues was only a small extent as compared to those induced by IR. Of note, we showed that 28 consecutive days of CRIS did not exacerbate IR effects (no additive effect with IR). These findings also suggest that studies on the concurrent exposure to PS and IR should be done using different endpoints in both short and long-term CRIS models.

Key words: Chronic restraint-induced stress; iron ion radiation; autophagy; endoplasmic reticulum stress

Introduction

Ionizing radiation (IR) has been widely used in many fields of medicine [1], and an increasing number of people have been faced with psychological stress (PS) [2], such as social [3] or restraint [4] stress.

It has been shown that IR and PS have deleterious effects on human health, and in particular, IR can cause severe mutations, carcinogenicity and toxicity [5]. Stress is the main risk factor in the etiology of

several psychiatric disorders, which increases anxiety and depression [6] and susceptibility to a variety of diseases, including hypertension, cardiovascular diseases, diabetes, and metabolic syndrome, and is a risk factor for cancer [7].

High linear energy transfer (LET) ions cause severe damage that is more difficult to repair than that caused by X- or γ-rays [8]. However, an increasing number of people are being exposed to high LET ions. Carbon ions are used in cancer radiotherapy [9]; the release of multiple radioisotopes increases the risk of exposure to radioactive contamination [10]; and high-atomic-number and high-energy ions are the main source of chronic whole body radiation upon astronauts [11]. Many patients with cancer who are undergoing radiotherapy suffer from PS including distress, anxiety and depression [12]. Fear of harmful health effects can restrict people's outdoor activities after a nuclear accident in which multiple radioisotopes are released and lead to radioactive contamination [13]. Astronauts are subjected to PS [14] and the risk of high background levels of IR [15] in restricted environments. Therefore, in future space missions, radiotherapy and nuclear accidents, protection strategies against the possible harmful effects of IR and PS are necessary. Thus, it is important to investigate whether PS alters the responses of humans to IR, and induces disease or toxicity so that we can understand the possible effects on human health.

Spermatogenesis is a complex process of male germ cell proliferation and maturation from spermatogonia to spermatozoa [16]. PS [17] and IR [18] cause testicular weight reduction and deterioration of spermatogenesis. Thus, it is important to investigate the effects of PS on IR-induced spermatogenesis dysfunction so that we can understand whether PS modifies testicular toxicity induced by IR and explore the underlying mechanisms of this toxicity in dysfunctional spermatogenesis. Here, we use an ^{56}Fe ion beam and chronic restraint on *Tp53*-heterozygous male mice to simulate the effects of PS on IR-induced reproductive health, and to detect the underlying mechanisms in the effects of PS responses on IR-induced toxicity in mouse testes. We focused on the roles of endoplasmic reticulum stress (ERS), apoptosis and autophagy in testicular injury, because ERS [19], apoptosis [20] and autophagy [21] play important roles in testicular injury and spermatogenesis dysfunction. However, the relationship among ERS, apoptosis and autophagy in the testes is still not clear, therefore, the aims of this study were to verify the relationship among ERS, autophagy and apoptosis in mouse testicular toxicity, and to explore whether the CRIS could cause any additive effect on induction of spermatogenesis dysfunction when concurrently exposed to IR.

Materials and methods

Animal treatment

Four-week-old C57BL/6N *Tp53*-heterozygous (*Trp53*$^{+/-}$) mice (BRC NO. 01361) were housed in an animal facility at the National Institute of Radiological Science (NIRS) of Japan. Two or one mice were housed in an autoclaved cage maintained at conventional temperature and humidity for 12 h light/12 h dark cycle (from 07:00 to 19:00 h), and allowed free access to standard laboratory chow (MB-1; Funabashi Farm Co., Japan) and acidified water (pH 3.0 ± 0.2). One week before the experiment, mice were randomly assigned to six experimental groups: control group (n=6), receiving neither restraint nor ^{56}Fe ion (IR); 0.1 Gy group (n=6) and 2 Gy group (n=6), receiving only ^{56}Fe ion radiation at 0.1 and 2.0 Gy, respectively; CRIS group (n=6), receiving only chronic restraint; CRIS+ 0.1 Gy group (n=7) and CRIS+2 Gy group (n=7), receiving chronic restraint and ^{56}Fe ion IR at 0.1 and 2.0 Gy, respectively. Chronic restraint, a well-established typical mouse model to induce PS, was applied to mice as described in our previous study [22]. Chronic restraint was performed using a flat-bottomed mouse rodent holder (RSTR541; Kent Scientific Co., USA) for 6 h/day for 28 consecutive days. Mice were placed daily in a restrainer and maintained horizontally in the cage during the 6-h restraint session (09:30–15:30 h) daily. Animals were then released into the same cage and were allowed to access freely food and water during the free session (15:30–09:30). The control, 0.1 Gy and 2 Gy groups received no restraint, but abstained from food and water from 09:30–15:30 as the CRIS, CRIS+0.1 Gy and CRIS+2 Gy groups during the 6-h restraint session each day. Three mice were put into an acrylic cylinder with three individual cells of the same size (each mouse in each cell) without anesthesia. The mice were in an air-breathing condition (there were six holes 5 mm in diameter in the wall of each cell). Total-body ^{56}Fe ion IR at 0.1 and 2.0 Gy (500 MeV/nucleon, 200 keV/μm) was delivered at dose rates of 0.085 Gy/min and 1.1–2.7 Gy/min, respectively, on the day 8 of the 28-day restraint regimen. ^{56}Fe ion irradiation was done at NIRS using Heavy Ion Medical Accelerator in Chiba (HIMAC). All experimental protocols involving mice were reviewed and approved by the Institutional Animal Care and Use Committee of NIRS.

Histology

At the end of the experiment, mice were anesthetized by the inhalation of carbon dioxide and then euthanized by cervical dislocation. Freshly collected testes were fixed in 4% paraformaldehyde and embedded in paraffin blocks, then sectioned at a 4 µm thickness. The sections were stained with hematoxylin and eosin (H & E) after paraffinization and rehydration. The stained sections were mounted and observed under a light microscope (Nikon 80i, Japan). Three sections were examined in each mouse [23].

Transmission electron microscopy (TEM)

Testes were cut into 1-mm³ blocks and immediately fixed in 2.5% glutaraldehyde phosphate for at least 24 h at room temperature and then kept at 4°C until embedded. Blocks were fixed in 1% osmium tetroxide for 2 h, dehydrated in ethanol and acetone, immersed in acetone, and embedded in epoxy resin. Ultrathin sections were cut to 50 nm and stained with uranyl acetate and lead citrate. TEM images were obtained using a FEI Tecnai G20 twin transmission electron microscopy (FEI Company, Hills-boro, OR) at 200 kV. Three mice were randomly selected from each group for ultrastructure observation [24].

TUNEL assay

Detection of apoptosis was done using a TUNEL assay kit (Beyotime, Shanghai, China). The sections were deparaffinized, hydrated and permeabilized with proteinase K at 37°C for 15 min and then treated with 3% hydrogen peroxide for 15 min to eliminate endogenous peroxidase activity. After washing with 0.01 M phosphate-buffered saline, the sections were incubated with the TUNEL reaction mixture (ratio of enzyme solution to labeling solution 1: 9) for 1 h at 37°C in a dark humidified atmosphere. The sections were incubated with transformant-POD (anti-fluorescein conjugated with carrot peroxidase) at 37°C for 30 min [25].

Immunoblotting

One testis was stored in 1 mL RNAlater™ stabilization solution (Invitrogen, Carlsbad, CA, USA) and kept at 4 °C until protein extracted. Total protein of testicular tissues (30 mg) was extracted using Trizol reagent (Invitrogen). Proteins were treated with a lysis buffer containing 7 mol/L urea, 2 mol/L thiourea, 4% (w/v) 3-[(3-cholamidopropyl)-dimethyl-ammonio]-1-propane sulfonate (Chaps), 2% (w/v) dithiothreitol (DTT) in the presence of 1% (w/v) protease inhibitor cock-tail (Sigma Chemical, St. Louis, MO, USA). Protein concentration was measured by the Bio-Rad Bradford protein assay with bovine serum albumin (Sigma) as a standard.

Forty microgram of testicular tissue protein samples were resolved by 10% and 12% SDS-PAGE. After electrophoresis, protein was transferred to a polyvinylidene difluoride membrane (PVDF) (Roche, Mannheim, Germany). The membranes were blocked with 5% skim milk (TBS with 5% nonfat milk powder) or 5% BSA (TBS with 5% BSA) for 2 h. Then the membrane was incubated with primary antibodies overnight at 4◦C. The primary antibodies were polyclonal anti-activated caspase 3 (Cat. no. BS7004), anti-Cytochrome c (Cat. no. BS1089), anti-GRP78 (Cat. no. BS6479), anti-Beclin 1 (Cat. no. AP0768) and anti-4EBP1 (Cat. no. BS6290) (1:1000, Bioworld technology, Inc, Ltd, Nanjing, China), anti-p62 (Cat. no. sc25523) and anti-LC3I (Cat. no. sc376404) (1:500, Santa Cruz, California, USA), anti-caspase-3 (Cat. no. 9662), anti-Akt (Cat. no. 4691T), anti-PI3 Kinase p85 (Cat. no. 4257T), anti-p70 S6 Kinase (Cat. no. 2708T), anti-phospho-mTOR (Cat. no. 5536T), anti-phospho-p70 S6 Kinase (Thr389) (Cat. no. 9234T), anti-phospho-PI3 Kinase p85 (Tyr458)/p55 (Tyr199) (Cat. no. 4228T), anti-phospho-Akt (Ser473) (Cat. no. 4060T) and anti-phospho-4EBP1 (Thr37/46) (Cat. no. 2855) (Cell signal, Boston, USA), anti-β-actin (Cat. no. ab8227), anti-Apaf1 (Cat. no. ab2001), anti-mTOR (Cat. no. ab32028), anti-Bax (Cat. no. ab32503), anti-Bcl-2 (Cat. no. ab182858), anti-APG5L/ATG5 (Cat. no. ab108327), anti-ATF4 (Cat. no. ab184909), anti-CHOP (Cat. no. ab179823), anti-eIF2α (Cat. no. ab5369) and anti-phospho-eIF2α (S51) (Cat. no. ab32157) (Abcam, Cambridge, UK), anti-PERK (Thr980) (Cat. no. bs2469R) and anti-phospho-PERK (Cat. no. bs3330R) (Cat. no. 3179) (Bioss Biotechnology, co, Ltd, Beijing, China), β-actin was used as a protein control to normalize volume of protein expression. After washing with TBST for 3 times, the membrane was incubated with secondary antibodies for 2 h in room temperature. The membrane was washed again and immunoreactivity was detected using an enhanced chemiluminescent HRP substrate kit (Cat. no. BLH01S050; Bioworld) and images were captured using a FluorChem 2 imaging system (Alpha Innotech, San Lean-dro, CA, USA). Protein bands from scanned images were quantified using the Quantity One 4.5.2 image analysis software (Bio-Rad). Data were corrected for background and expressed as optical density (OD/mm²).

Immunohistochemistry

Four µm of testicular sections was deparaffinized and rehydrated. After finishing antigen retrieval, sections were incubated in 1% Triton X-100 for 30 min, and then incubated for 10 min in 3% (vol/vol) H_2O_2 in methanol. The sections were blocked with 5% BSA (5 g BSA in 100 mL TBS) for 30

min, then were applied with primary antibody anti-GRP78, anti-activated caspase 3 and anti-Cytochrome c (1:100, Bioworld), anti-p62 (1:100, Santa cruz), anti-Atg5 and CHOP (1:100, Abcam). Biotinylated goat anti-rabbit immunoglobulin antibody and a Streptavidin-Peroxidase kit (Bioss) were used as second- and the third-phase reagents, respectively. Diaminobenzidine (DAB) (Bioss) was used for detection and hematoxylin was used for counterstaining. The samples were then dehydrated and mounted for observation using a light microscope (Nikon 80i, Japan).

Statistical analysis

SPSS version 19.0 (SPSS Inc., Chicago, IL, USA) was used to analyze the differences based on one-way analysis of variance and Duncan's post hoc test. Values were expressed as mean ± SEM. A p level ≤ 0.05 was considered statistically significant.

Results

IR and CRIS+IR reduced testicular weight and relative weight of the testes in *Trp53*^{+/−} mouse testes

The effects of IR and CRIS+IR on testicular weight and relative weight of the testes (testes weight/body weight) are shown in Table 1. Significant decreases in testicular weight and relative weight of the testes were observed in the IR and CRIS+IR groups. Compared with the controls, there was no significant difference between the CRIS+IR and IR groups (compared at the same [56]Fe ion dose), and there were no significant changes in testicular weight and relative weight of the testes in the CRIS group.

Table 1. Comparison of body weight and relative weight of the testes in *Trp53*^{+/−} mice.

| Group	Testes weight (g)	Relative weight of the testes (%)
Control (n=6)	0.2107±0.005	0.708±0.0236
0.1 Gy (n=6)	0.176±0.0091**	0.5891±0.0272***
2 Gy (n=6)	0.08717±0.0039***	0.3011±0.0802***
CRIS (n=6)	0.1982±0.0055	0.768±0.1221
CRIS+0.1 Gy (n=7)	0.1645±0.009***	0.6394±0.0779*
CRIS+2 Gy (n=7)	0.079±0.0035***	0.3117±0.1121***

Values represent the average ± S.E.M. Asterisks indicate a statistically significant difference from control: * P < 0.05, ** P < 0.01, *** P < 0.001 on one-way ANOVA with Duncan's post hoc analysis.

IR and CRIS+IR induced histological injury in *Trp53*^{+/−} mouse testes

The normal testicular structure of spermatogenesis showed that the seminiferous tubules were smooth and the arrangement of spermatogenic cells was regular. The testicular structure of the CRIS group had only small changes, with reduction in thickness of the spermatogenic epithelium. However, in the IR and CRIS+IR groups, the testes showed obvious pathological changes compared with the control group. The spermatogenic epithelium was severely damaged, spermatogenic cells were arranged in a disordered manner, the number of spermatogonia decreased and the thickness of epithelium was reduced significantly. Vacuolization was present in the spermatogenic epithelium, and in particular, this alteration was more significant in the CRIS+2 Gy and 2 Gy groups (Fig. 1).
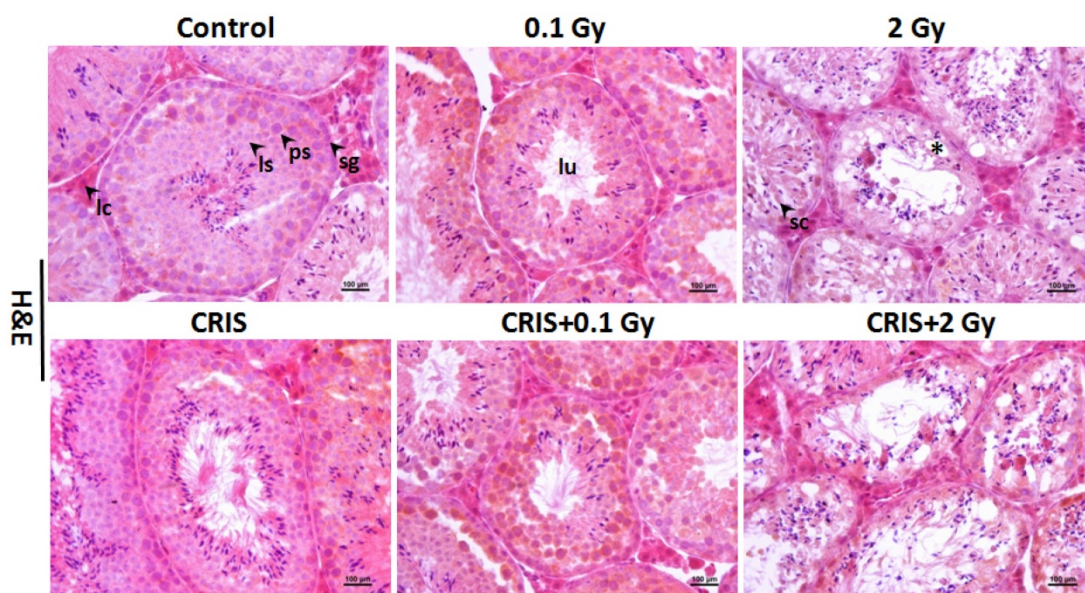
Figure 1. Testes histopathology stained with H&E in *Trp53*^{+/−} mouse testes (magnification, 200×; scale bar = 100 μm), arrows indicate spermatogenic cells in the seminiferous tubule (lu, lumen; sg, spermatogonia; ps, pachytene spermatocyte; ls, leptotene stage spermatocyte), severe vacuolization of spermatogenic cells in the seminiferous tubule (*). CRIS, chronic restraint-induced stress.
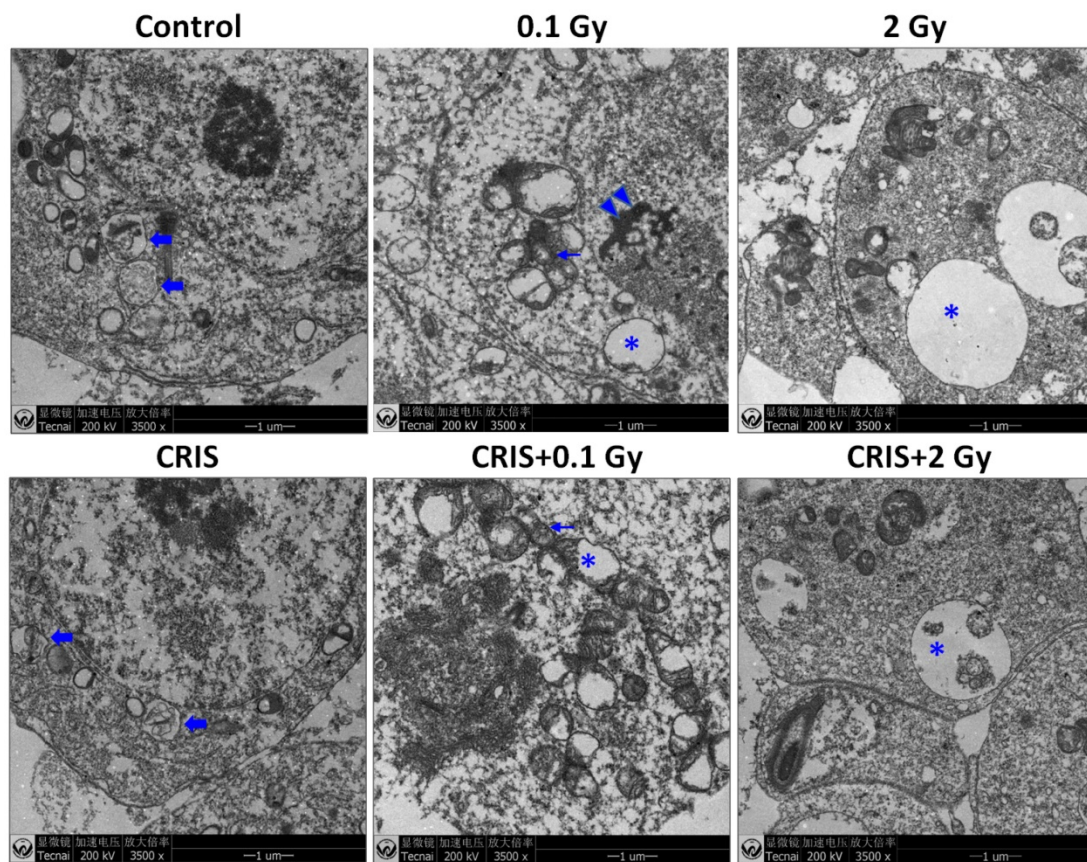
Figure 2. The ultrastructural abnormalities in *Trp53*^+/− mouse testes. Representative transmission electron microscopy images of each group. The asterisks indicate focal vacuolation; the double arrow heads indicate apoptosis including condensation and margination of nuclear chromatin; the thin arrows indicate swollen mitochondria with the degeneration or loss of cristae; the fold arrows indicate autophagosomes. CRIS, chronic restraint-induced stress.

IR and CRIS+IR induced ultrastructural abnormalities in *Trp53*^+/− mouse testes

Transmission electron microscopy (TEM) showed the testicular ultrastructure in the control group (Fig. 2). Compared with control group, IR and CRIS+IR caused extensive abnormalities in testicular tissue: vacuolation and swollen degenerated mitochondria. Apoptotic characteristics were seen, including condensation and margination of nuclear chromatin. Autophagosome-like structures (containing degraded organelles and other cytoplasmic contents) appeared in the cytoplasm of spermatogenic cells in the control group, although they were not so frequent in the IR and CRIS+IR groups.

IR and CRIS+IR induced apoptotic spermatogenic cells in *Trp53*^+/− mouse testes

To assess further the incidence of apoptotic spermatogenic cells in the *Trp53*^+/− mouse testes, TUNEL assay was performed to evaluate the apoptotic spermatogenic cells. The apoptotic signal is shown in Fig. 3A, there were almost no apoptotic cells in the spermatogenic epithelium in the control group; only a few apoptotic Leydig cells were found, while the degree of apoptotic cells in the CRIS group was slight, and the apoptotic cells were mainly pachytene and leptotene stage spermatocytes. However, in the IR and CRIS+IR groups, almost all types of testicular cells showed signs of apoptosis, including spermatogonia, pachytene spermatocytes, leptotene spermatocytes, spermatozoa and Leydig cells. In particular, in the CRIS+2 Gy and 2 Gy groups, radiation-resistant Sertoli cells showed signs of apoptosis. To confirm the apoptotic pathway, apoptosis-related marker proteins were determined with Western blotting. Compared with the controls, expression levels of Apaf 1, cytochrome c, activated-caspase 3 and Bax/Bcl-2 were dramatically increased in the CRIS+IR and IR groups. There was no significant difference between the CRIS+IR and IR groups (compared at the same ^56Fe ion dose). There were significant changes in Bax/Bcl-2, cytochrome-c and caspase 3 in the CRIS group (Fig. 3B, 3C). In support of the results of Western blotting immunohistochemistry also revealed strong cytoplasmic staining for cytochrome c and activated-caspase 3 in the testes, especially in the spermatogonia and pachytene and leptotene spermatocytes in the CRIS+2 Gy and 2 Gy groups (Fig. 3D). This indicated that cytochrome c was released from the mitochondria to

the cytoplasm and caspase 3 was activated. These results suggest that both IR and CRIS+IR can induce apoptosis of spermatogenic cells, and there was no significant difference in the degree of apoptosis between the CRIS+IR and IR groups (compared at the same ^{56}Fe ion dose).
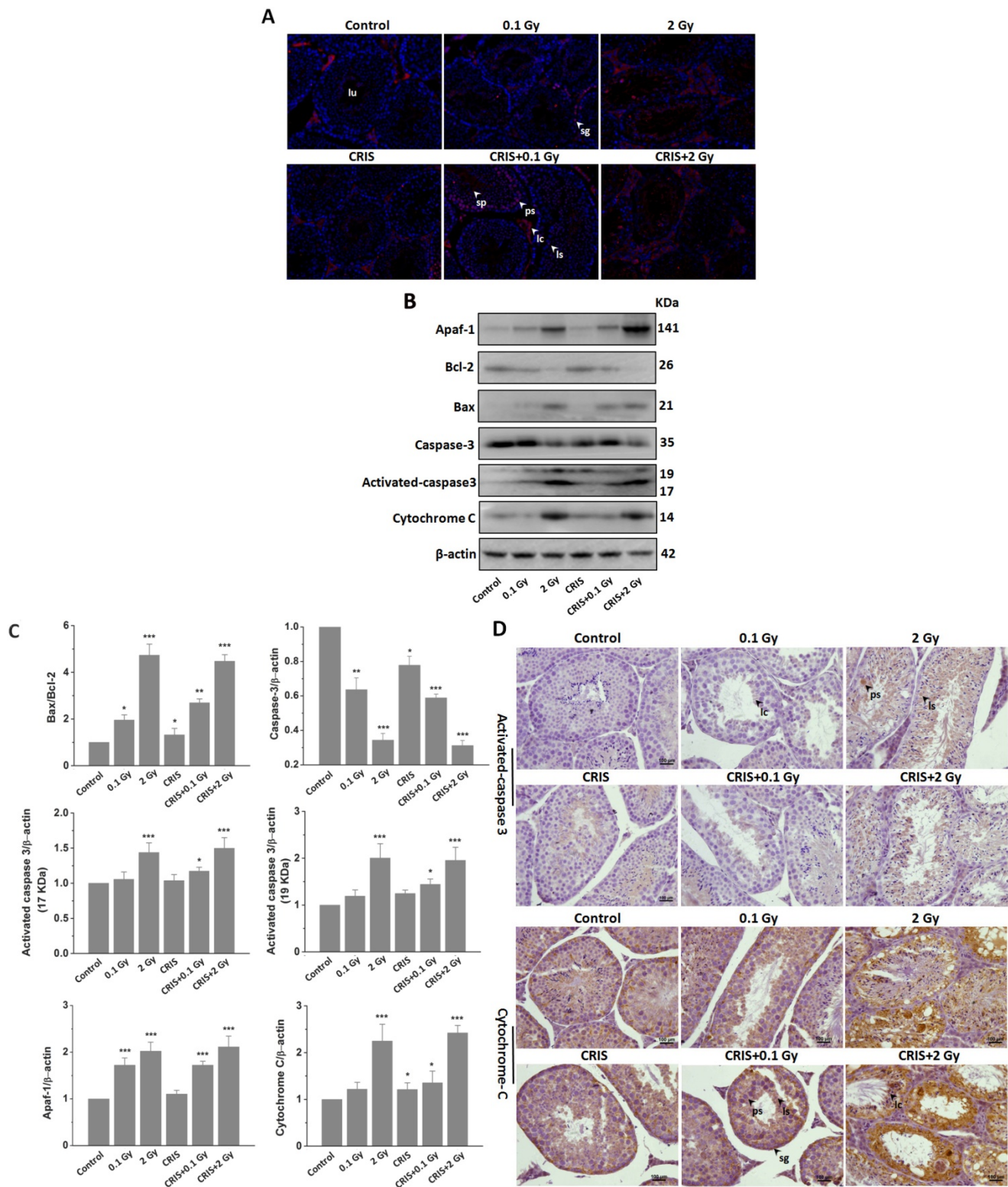
Figure 3. The analysis of apoptosis pathways in *Trp53$^{+/-}$* mouse testes. (A) Apoptotic spermatogenic cells stained with TUNEL in *Trp53$^{+/-}$* mouse testes (magnification, 200×; scale bar = 100 μm), arrows indicate TUNEL-positive cells (red) in the seminiferous tubule (lu, lumen; sg, spermatogonia; ps, pachytene spermatocyte; ls, leptotene stage spermatocyte; lc, leydig cell; sp, spermatozoa). (B) Representative images of Western blotting for Apaf-1, bax, bcl-2, cytochrome c, caspase-3 and activated caspase-3 in *Trp53$^{+/-}$* mouse testes of each group. (C) Relative each protein expression compared with control; Values represent the average ± S.E.M from three gels per group. Asterisks indicate a statistically significant difference from control: * $P < 0.05$, ** $P < 0.01$, *** $P < 0.001$ on one-way ANOVA with Duncan's post hoc analysis. (D) Representative images of activated caspase-3 and cytochrome c-stained in each group. sg, spermatogonia; ps, pachytene spermatocyte; ls, leptotene stage spermatocyte; lc, leydig cell; CRIS, chronic restraint-induced stress.
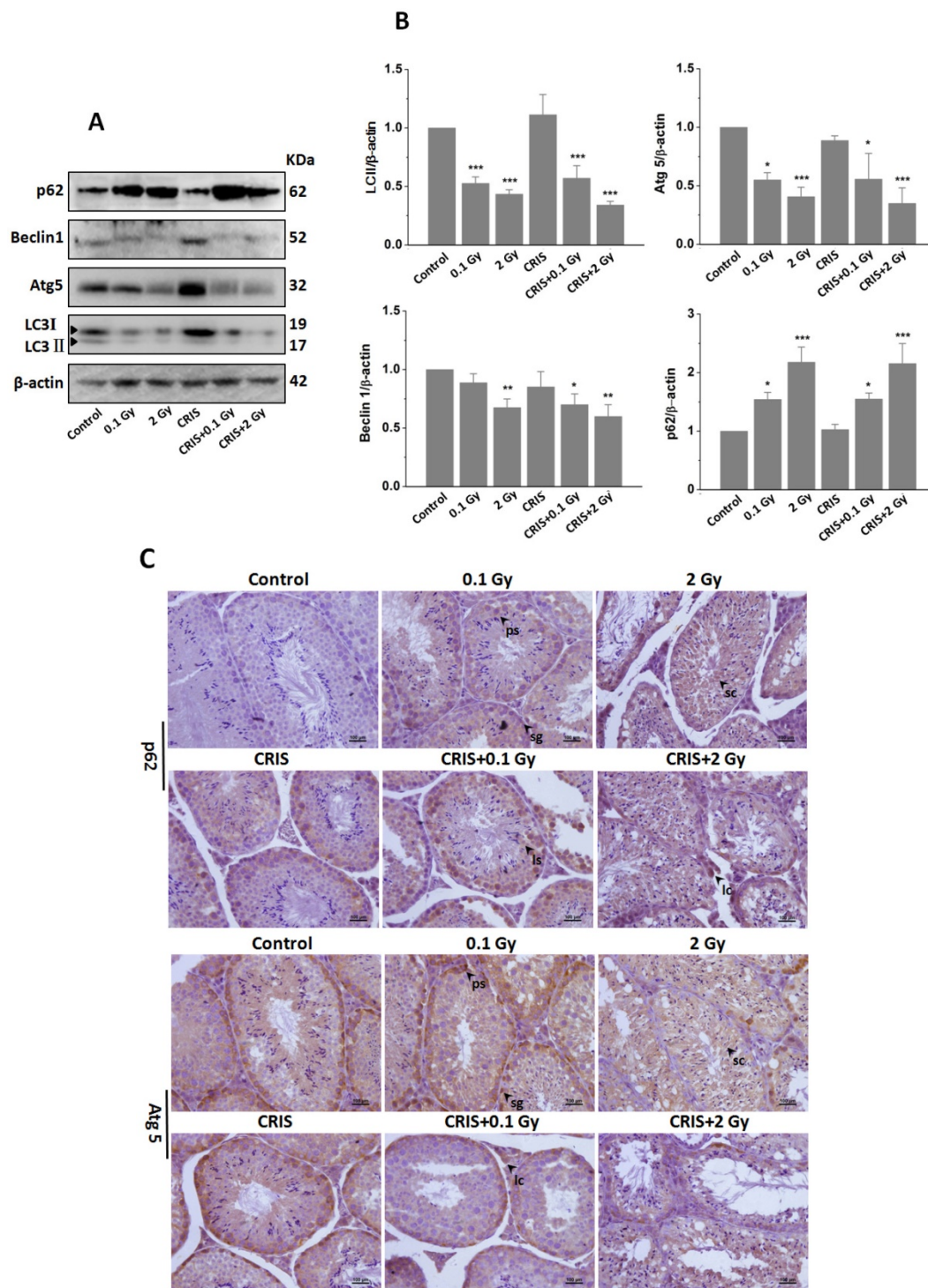
Figure 4. The analysis of autophagy proteins in *Trp53*$^{+/-}$ mouse testes. (A) Representative images of Western blotting for LC3 II, Beclin1, Atg5 and p62 in *Trp53*$^{+/-}$ mouse testes of each group. (B) Relative each protein expression compared with control; Values represent the average ± S.E.M from three gels per group. Asterisks indicate a statistically significant difference from control: * $P < 0.05$, ** $P < 0.01$, *** $P < 0.001$ on one-way ANOVA with Duncan's post hoc analysis. (C) Representative images of Atg5 and p62-stained in each group. sg, spermatogonia; ps, pachytene spermatocyte; ls, leptotene stage spermatocyte; lc, leydig cell; sc, Sertoli cell; CRIS, chronic restraint-induced stress.

IR and CRIS+IR inhibited autophagic formation in *Trp53*$^{+/-}$ mouse testes

TEM revealed autophagic formation in *Trp53*$^{+/-}$ mouse testes. Autophagosome-like structures (containing degraded organelles and other cytoplasmic contents) appeared in the cytoplasm of spermatogenic cells in the control group; however, they were almost absent in the CRIS+IR groups (Fig. 2). TEM showed different autophagosome formation. To confirm the changes in autophagy, we tested whether autophagy was inhibited in mouse testes by IR and CRIS+IR through analyzing autophagy markers including Beclin-1, LC3, Atg5 and p62 (Fig. 4A). Compared with

the controls, protein expression of LC3II, Beclin-1 (not including the 0.1 Gy group) and Atg5 was decreased and p62 expression was increased in the IR and CRIS+IR groups. There was no significant difference between the CRIS+IR and IR groups (compared at the same ^{56}Fe ion dose), and there were no significant changes in these proteins in the CRIS group (Fig. 4B, 4C). These results were also accompanied by weak staining of Atg5 and strong staining of p62 in testicular cells in the IR and CRIS+IR groups (Fig. 4C), suggesting that autophagosome formation was inhibited.

IR and CRIS+IR inhibited autophagic formation through activating PI3K/AKT/mTOR pathway

The PI3K/AKT/mTOR signaling pathway plays a key role in driving autophagy [26], therefore, we investigated whether it was involved in IR and CRIS+IR autophagy inhibition. Compared to the controls, phosphorylation of phosphoinositide 3-kinase (PI3K), AKT, mammalian target of rapamycin (mTOR), p70S6 K and 4EBP1 was increased in the IR and CRIS+IR groups, and there were no obvious changes in the CRIS group (Fig. 5A,

5B and 5C). There was no significant difference between the CRIS+IR and IR groups (compared at the same ^{56}Fe ion dose) (Fig. 5C). These results suggest that IR and CRIS+IR exert an active effect on PI3K/AKT/mTOR signaling to inhibit autophagic formation.

IR and CRIS+IR induced ERS in *Trp53*$^{+/−}$ mouse testes

To investigate ERS after CRIS+IR, we analyzed protein expression of markers GRP78 (78-kDa glucose-regulated protein) and C/EBP homologous protein (CHOP) in testes. Compared to the controls, there was a significant increase in protein levels of GRP78 and CHOP in the IR and CRIS+IR groups, and there were no obvious changes in the CRIS group (Fig. 6A, 6B). GRP78 and CHOP expression did not differ significantly between the CRIS+IR and IR groups (compared at the same ^{56}Fe ion dose) (Fig. 6A, 6B). Immunohistochemical analysis revealed that GRP78 and CHOP increased mainly in the spermatogonia and spermatocytes. These results suggest that IR and CRIS+IR induced ERS in testes.
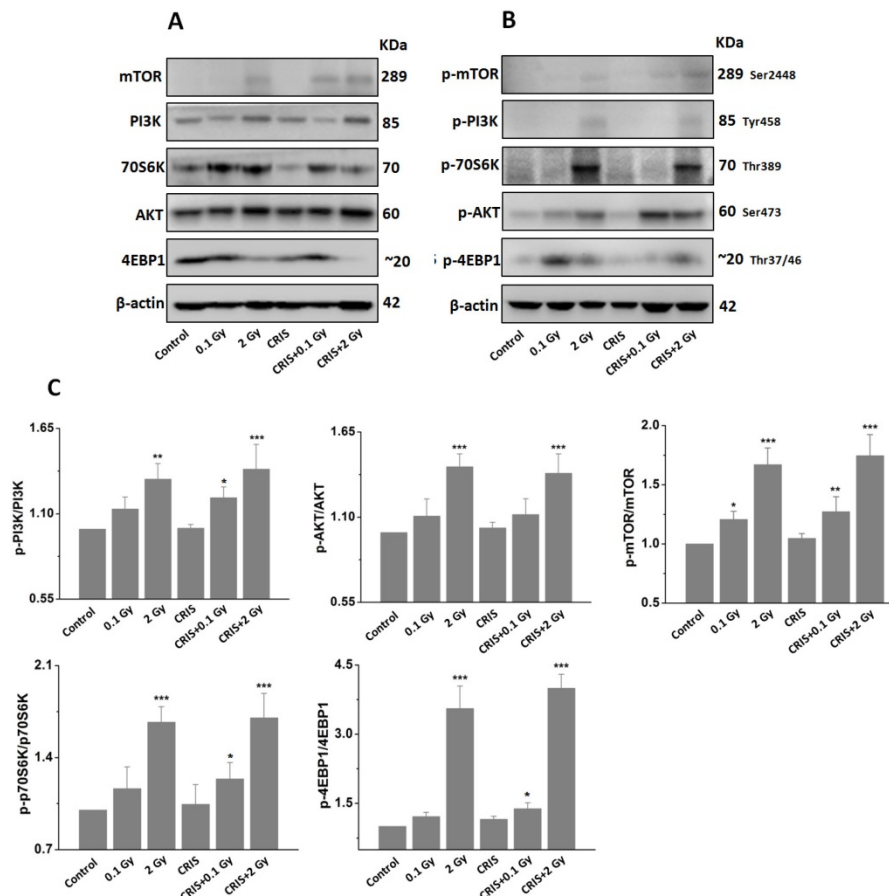
Figure 5. The analysis of PI3K/AKT/mTOR pathway in *Trp53*$^{+/−}$ mouse testes. (A) Representative images of Western blotting for PI3K, AKT, mTOR, 70S6K and 4EBP1 in *Trp53*$^{+/−}$ mouse testes of each group. (B) Representative images of Western blotting for phospho-PI3K, phospho-AKT, phospho-mTOR, phospho-70S6K and phospho-4EBP1 in *Trp53*$^{+/−}$ mouse testes of each group. (C) Relative each protein expression compared with control; Values represent the average ± S.E.M from three gels per group. Asterisks indicate a statistically significant difference from control: * P < 0.05, ** P < 0.01, *** P < 0.001 on one-way ANOVA with Duncan's post hoc analysis.
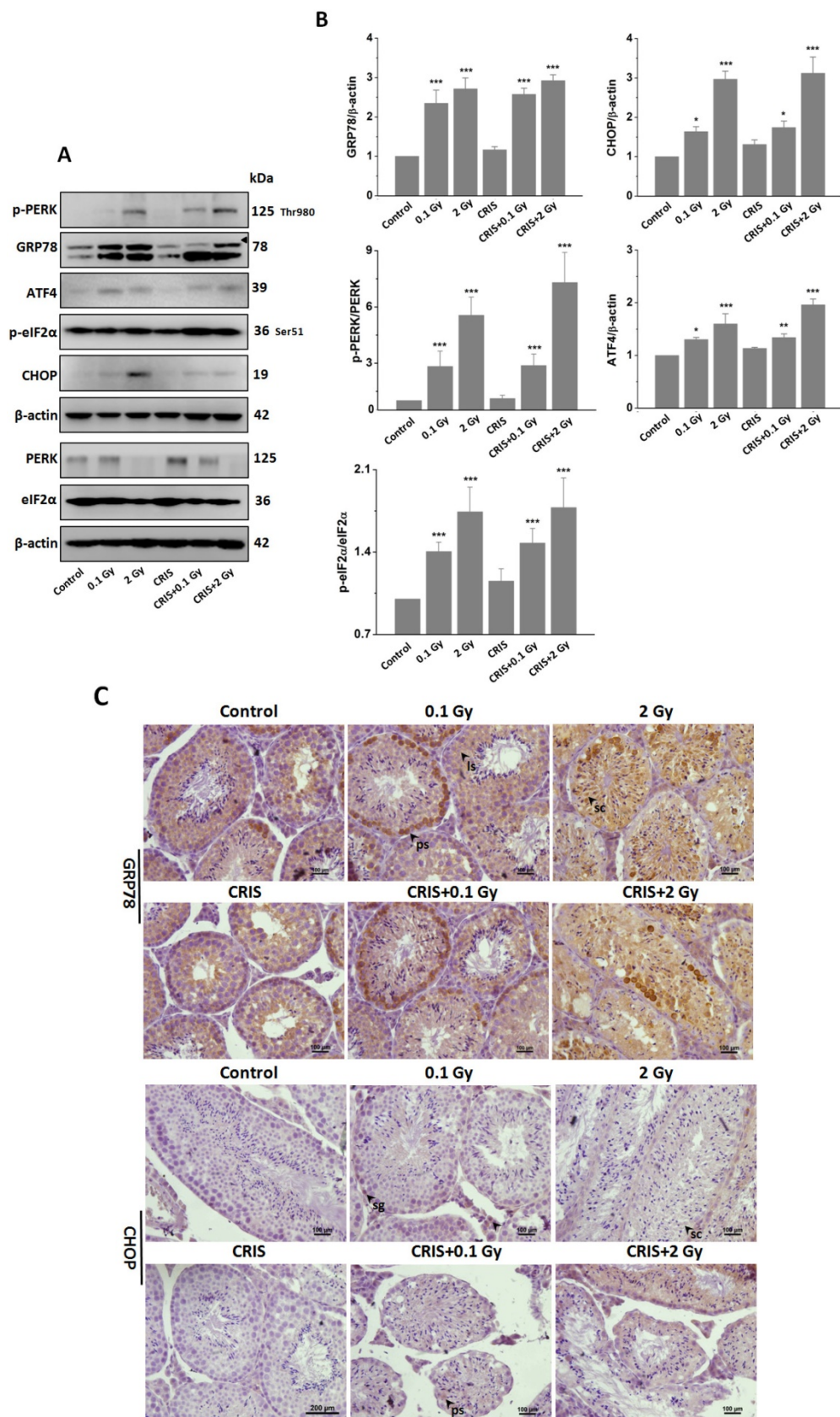
Figure 6. The analysis of endoplasmic reticulum stress markers GRP78 and CHOP, and PERK-eIF2α-ATF4 pathway in *Trp53*^{+/−} mouse testes. (A) Representative images of Western blotting for GRP78, CHOP, PERK, eIF2α, phospho-PERK, phospho-eIF2α and ATF4 in *Trp53*^{+/−} mouse testes of each group. (B) Relative each protein expression compared with control; Values represent the average ± S.E.M from three gels per group. Asterisks indicate a statistically significant difference from control: * P < 0.05, ** P < 0.01, *** P < 0.001 on one-way ANOVA with Duncan's post hoc analysis. (C) Representative images of GRP78 and CHOP-stained in each group. sg, spermatogonia; ps, pachytene spermatocyte; ls, leptotene stage spermatocyte; lc, leydig cell; sc, Sertoli cell; CRIS, chronic restraint-induced stress.

IR and CRIS+IR induced ERS through activating PERK-eIF2α-ATF4 pathway

PERK is the main signal of ERS. The PERK signaling pathway with eukaryotic translation initiation factor (eIF) 2α, ATF4 and other downstream factors are up-regulated by ERS [27]. We analyzed the PERK/eIF2α/ATF4 pathway by Western blotting. Compared to the controls, IR and CRIS+IR increased protein expression of p-PERK, p-eIF2α and ATF4, and there were no obvious changes in the CRIS group (Fig. 6A, 6B). The expression levels of PERK/eIF2α/ATF4 pathway proteins showed no significant difference between the CRIS+IR and IR groups (compared at the same ^{56}Fe ion dose) (Fig. 6A, 6B). These results indicate that IR and CRIS+IR induced ERS through activating the PERK/eIF2α/ATF4 pathway.

Discussion

The goals of this study were to investigate the effects of high LET particle irradiations on the testes, and whether CRIS modifies spermatogenesis dysfunction induced by IR, and to clarify the mechanism of apoptosis induction by IR and CRIS+IR in *Trp53*$^{+/-}$ mouse testes.

We observed significant decreases in testicular weight and relative weight of the testes, indicating the deleterious consequences of IR and CRIS+IR. We monitored the changes in mitochondrial apoptotic pathways after IR and CRIS+IR exposure. Cytochrome c is a key inducer of apoptosis, which binds to Apaf-1 in the cytosol to activate caspase-3 [28], and is released from mitochondria by Bcl-2 family proteins binding to the mitochondrial membrane [29]. Immunohistochemistry showed that apoptotic cells are mainly pachytene and leptotene spermatocytes and Sertoli cells, indicating that IR and CRIS+IR damaged spermatogenesis and induced testicular cell apoptosis. Our study showed that IR and CRIS+IR significantly increased cytochrome c, Apaf-1, activated caspase-3 and Bax expression but markedly suppressed Bcl-2. These results demonstrated the crucial role of the mitochondria-dependent pathway in spermatogenic cell apoptosis induced by IR and CRIS+IR, that IR and CRIS+IR disturbed mitochondrial dysfunction, and induced mitochondrial cytochrome c release to activate caspase-3 in spermatogenic cell apoptosis. The expression of these proteins had no significant difference between the CRIS+IR and IR groups (compared at the same ^{56}Fe ion dose). On the other hand, the expression of Bax/Bcl-2, caspase 3 and cytochrome c was significantly different in the CRIS groups compared with the controls. Consistently, histological and TUNEL analyses revealed that CRIS alone can induce reduction in the thickness of spermatogenic epithelium and apoptosis in Leydig cells. However, the extent of theses pathological and molecular changes in testicular tissues induced by CRIS alone was very limited as compared to that induced by IR. These results indicated that CRIS did not enhance apoptosis in *Trp53*$^{+/-}$ mouse testes treated with IR and apoptosis was mainly induced by IR.

In this study, the ERS was analyzed after CRIS+IR exposure, because ERS is an important factor in cell death [19]. BIP, also known as GRP78, is a chaperone protein located in the ER and its expression significantly increases when ERS occurs [30]. The transcription factor CHOP is a key participant in the ERS-activated apoptotic pathway [31]. We showed that GRP78 and CHOP proteins were overexpressed, which suggests that the ERS apoptotic pathway can be activated by IR and CRIS+IR. To confirm this mechanism, we analyzed the PERK/eIF2α/ATF4/CHOP pathway. PERK is an ER-resident transmembrane protein and plays an important role in apoptosis [32]. ERS activates PERK, phosphorylates eIF2α, and inhibits translation of mRNA into protein. ATF4 is activated by phosphorylating eIF2α and induces CHOP expression [33]. Following IR and CRIS+IR exposure, expression of p-PERK, p-eIF2α, ATF4 and CHOP was upregulated, suggesting that IR and CRIS+IR activate the PERK/eIF2a/ATF4/CHOP pathway resulting in apoptosis and testicular damage. Expression of ERS proteins was not significantly between the CRIS and control groups, nor between the CRIS+IR and IR groups (compared at the same ^{56}Fe ion dose). These results indicated that CRIS did not enhance ERS in *Trp53*$^{+/-}$ mouse testes treated with IR and ERS was mainly induced by IR.

Some studies have confirmed the key role of autophagy in male reproductive dysfunction [34]. However, there is no study about autophagy in testes after CRIS+IR treatment. Beclin-1 is required for autophagosome formation and autolysosomal fusion [35], and LC3II is required for autophagosome formation [36]. Atg5 is necessary for autophagosome extension [37]. p62 is incorporated into autophagosomes and degraded in lysosomes after fusion with the autophagosomes, and its accumulation reflects autophagosome formation and degradation is blocked [38]. In the present study, we found that IR and CRIS+IR significantly decreased the content of LC3-II, Atg5 and Beclin 1, and increased p62 in mouse testes, indicating that IR and CRIS+IR inhibit autophagosome formation, leading to p62 accumulation. To combine these results, we monitored autophagic vacuoles in the cytoplasm using TEM, and we could hardly see any autophagic vacuoles in the IR and CRIS+IR groups. Taken together, these data indicate that IR and CRIS+IR

inhibit autophagy via inhibiting autophagosome formation in mouse testes. The expression of autophagic marker proteins including LC3, Beclin-1, Atg5 and p62 did not differ significantly between the CRIS and control groups, nor between the CRIS+IR and IR groups (compared at the same [56]Fe ion dose), which indicated that CRIS did not exacerbate inhibition on autophagosome formation in *Trp53*^{+/−} mouse testes treated with IR. To confirm the mechanism by which IR and CRIS+IR inhibit autophagy via inhibiting autophagosome formation, we compared the PI3K/AKT/mTOR pathway, because the role of this pathway in modulation of cell autophagy has been demonstrated [39]. Activated PI3K can promote the activation of Akt and then modulate the mTOR signaling pathway [40]. mTOR is a central checkpoint that negatively regulates autophagy, and inhibition of the mTOR/p70S6K axis can activate autophagy [41]. In this study, IR and CRIS+IR phosphorylated mTOR, p70S6K and 4EBP1 in mouse testes, indicating that mTOR signaling was activated by IR and CRIS+IR and inhibited autophagy. This suggests that inhibition of autophagy in mouse testes is mediated by activation of the PI3K/AKT/mTOR pathway. Western blotting showed that expression of PI3K/AKT/mTOR pathway proteins did not differ significantly between the CRIS and control groups, and these proteins did not differ significantly between the CRIS+IR and IR groups (compared at the same [56]Fe ion dose), which provides evidence that CRIS did not exacerbate inhibition on autophagy in *Trp53*^{+/−} mouse testes treated with IR.

We used the *Tp53*-heterozygous mouse model to mimic the effects of CRIS responses on [56]Fe ion radiation, because the CRIS is a risk factor for γ-radiation-induced carcinogenesis in *Trp53*^{+/−} mice [42]. Therefore, we should pay more attention to the effects of PS on IR-induced toxicity in testes, because, testes are one of the most sensitive organs to PS [17] and IR [18]. Although CRIS enhanced γ-radiation-induced carcinogenesis in *Trp53*^{+/−} mice, the results of the present study showed that CRIS did not enhance testicular cell apoptosis induced by IR. Moreover, in the present study, the control group showed high autophagy and low apoptosis, which could be related to the heterozygous *Trp53*, because inhibition of p53 leads to autophagy [43]. We used chronic periodic restraint on a daily basis for 6 h for 28 consecutive days. All results showed there were no marked changes in apoptosis, ERS and autophagy level in the CRIS groups, which could be related to restraint time, because spermatogenesis is a dynamic process and has potent capacity for recovery in spermatogenic cells if circumstances change. However, it does mean that PS has the potential to cause harm to the testes, therefore, we need to improve the restraint model and extend the restraint time in future studies.

In this study, ERS played a key role in apoptosis activation and autophagy inhibition, because it displayed dual-directional effects in regulating cell function under cellular stress, and some crosstalk elements played important roles in these processes [44]. CHOP is a major factor in ERS-induced cell death. ERS activated CHOP and induced apoptosis by attenuating Bcl-2 [45], meanwhile, Bax combines with Bcl-2 to attenuate cell survival function and induce apoptosis [46]. ERS activated caspase-3 and then caused apoptotic cell death [47]. Combination of these previous studies and our results show that IR and CRIS+IR can cause ERS in mouse testes, activate crosstalk elements of apoptosis, and induce testicular cells apoptosis. mTOR plays an important role in regulation of autophagy and apoptosis under ERS; ERS activates mTOR, promotes apoptosis and inactivates autophagy [48]. Therefore, in the present model, we concluded that CRIS was not an additive factor with IR compared with IR alone in inhibition of autophagy and enhancement of ERS-induced apoptosis in *Trp53*^{+/−} mouse testes, because most results showed no significant difference between the CRIS+IR and IR groups (compared at the same [56]Fe ion dose). Further studies should be done to verify the effect of concurrent exposure to both PS and IR using a longer-term CRIS model.

In summary, the present study shows that IR and CRIS+IR can cause injury and spermatogenesis disorder in mouse testes, and that ERS is activated by IR and CRIS+IR via activation of the PERK/eIF2α/ATF4/CHOP pathway, and increasing apoptosis of spermatogenic cells. Autophagy is inhibited by IR and CRIS+IR via activation of the PI3K/AKT/mTOR pathway under ERS, and decreasing the survival of spermatogenic cells. There was no difference in these results between the CRIS+IR and IR groups, which shows that IR inhibited autophagy and enhanced ERS-induced apoptosis in *Trp53*^{+/−} mouse testes, and CRIS was not an additive factor with IR compared with IR alone. These results provide a new perspective for understanding the causes of testicular toxicity induced by IR and CRIS+IR. Moreover, we concluded that 28 consecutive days of CRIS had no additive effects with IR compared with IR alone in causing testicular toxicity. These findings also suggest that investigations on the concurrent exposure to PS and IR should be done using different endpoints in both short and long-term PS models.

Acknowledgments

Abbreviations

CRIS: Chronic restraint-induced stress; IR: Ionizing diation; PS: Psychological stress; *Trp53$^{+/-}$*: *Trp53*-heterozygous; HIMAC: Heavy Ion Medical Accelerator in Chiba; TEM: Transmission electron microscopy; PBS: phosphate buffered saline; PVDF: polyvinylidene difluoride membrane; DAB: Diaminobenzidine; NIRS: National Institute of Radiological Sciences.

Competing Interests

The authors have declared that no competing interest exists.

References

[1] Kwon JE, Kim BY, Kwak SY, Bae IH, Han YH. Ionizing radiation-inducible microRNA miR-193a-3p induces apoptosis by directly targeting Mcl-1. Apoptosis. 2013; 18: 896-909.

[2] Goyal M, Singh S, Sibinga EM, Gould NF, Rowland-Seymour A, Sharma R, Berger Z, Sleicher D, Maron DD, Shihab HM, Ranasinghe PD, Linn S, Saha S, Bass EB, Haythornthwaite JA. Meditation programs for psychological stress and well-being: a systematic review and meta-analysis. JAMA. Intern. Med. 2014; 174: 357-368.

[3] Kataoka N, Hioki H, Kaneko T, Nakamura K. Psychological stress activates a dorsomedial hypothalamus-medullary raphe circuit driving brown adipose tissue thermogenesis and hyperthermia. Cell Metab. 2014; 20: 346-358.

[4] Iwata M, Ota KT, Li XY, Sakaue F, Li N, Dutheil S, Banasr M, Duric V, Yamanashi T, Kaneko K, Rasmussen K, Glasebrook A, Koester A, Song D, Jones KA, Zorn S, Smagin G, Duman RS. Psychological stress activates the inflammasome via release of adenosine triphosphate and stimulation of the purinergic type 2X7 receptor. Biol. Psychiatry. 2016; 80: 12-22.

[5] Morgan WF, Sowa MB. Non-targeted effects induced by ionizing radiation: mechanisms and potential impact on radiation induced health effects. Cancer Lett. 2015; 356: 17-21.

[6] Dong L, Wang S, Li Y, Zhao Z, Shen Y, Liu L, Xu G, Ma C, Li S, Zhang X, Cong B. RU486 reverses emotional disorders by influencing astrocytes and endoplasmic reticulum stress in chronic restraint stress challenged rats. Cell. Physiol. Biochem. 2017; 42: 1098-1108.

[7] Schoenfeld TJ, McCausland HC, Morris HD, Padmanaban V, Cameron HA. Stress and loss of adult neurogenesis differentially reduce hippocampal volume. Biol. Psychiatry. 2017; S0006-3223: 31585-31588.

[8] Duan X, Zhang H, Liu B, Li XD, Gao QX, Wu ZH. Apoptosis of murine melanoma cells induced by heavy-ion radiation combined with Tp53 gene transfer. Int. J. Radiat. Biol. 2008; 84: 211-217.

[9] Li HY, He Y, Di C, Yan J, Zhang H. Comparative analysis of the serum proteome for biomarker discovery to reveal hepatotoxicity induced by iron ion radiation in mice. Life. Sci. 2016; 167: 57-66.

[10] Leon GR. Overview of the psychosocial impact of disasters. Prehosp. Disaster. Med. 2004; 19: 4-9.

[11] Zeitlin C, Hassler D, Cucinotta F, Ehresmann B, Wimmer-Schweingruber R, Brinza D, Kang S, Weigle G, Böttcher S, Böhm E. Measurements of energetic particle radiation in transit to Mars on the Mars Science Laboratory. Science. 2013; 340: 1080-1084.

[12] Cordes MC, Scherwath A, Ahmad T, Cole AM, Ernst G, Oppitz K, Lanfermann H, Bremer M, Steinmann D. Distress, anxiety and depression in patients with brain metastases before and after radiotherapy. BMC Cancer. 2014; 14: 731.

[13] Boice JDJr. Radiation epidemiology: a perspective on Fukushima. J. Radiol. Prot. 2012; 2012: N33-40.

[14] Basner M, Dinges DF, Mollicone DJ, Savelev I, Ecker AJ, Di Antonio A, Jones CW, Hyder EC, Kan K, Morukov BV, Sutton JP. Psychological and behavioral changes during confinement in a 520-day simulated interplanetary mission to mars. PLoS One. 2014; 9: e93298.

[15] Yatagai F, Ishioka N. Are biological effects of space radiation really altered under the microgravity environment. Life. Sci. Space. Res. 2014; 3: 76-89.

[16] Hai Y, Hou J, Liu Y, Liu Y, Yang H, Li Z, He Z. The roles and regulation of Sertoli cells in fate determinations of spermatogonial stem cells and spermatogenesis. Semin. Cell. Dev. Biol. 2014; 29: 66-75.

[17] Nirupama M, Devaki M, Nirupama R, Yajurvedi HN, Chronic intermittent stress-induced alterations in the spermatogenesis and antioxidant status of the testis are irreversible in albino rat. J. Physiol. Biochem. 2013; 69: 59-68.

[18] Zhang H, Zhao W, Wang Y. Induction of cytogenetic adaptive response in spermatogonia and spermatocytes by pre-exposure of mouse testis to low-dose 12C6+ ions. Mutat Res. 2008; 653: 109-112.

[19] Pluquet O, Pourtier A, Abbadie C. The unfolded protein response and cellular senescence. A review in the theme: cellular mechanisms of endoplasmic reticulum stress signaling in health and diseas. Am. J. Physiol. Cell. Physiol. 2015; 308: C415-25.

[20] Huang KH, Weng T, Huang HY, Huang KD, Lin WC, Chen SC, Liu SH. Honokiol attenuates torsion/detorsion-induced testicular injury in rat testis by way of suppressing endoplasmic reticulum stress-related apoptosis. Urology. 2012; 79: 967.e5-11.

[21] Li HY, He Y, Zhang H, Miao G. Differential proteome and gene expression reveal response to carbon ion irradiation in pubertal mice testes. Toxicol. Lett. 2014; 225: 433-444.

[22] Wang B, Tanaka K, Katsube T, Ninomiya Y, Vares G, Liu Q, Morita A, Nakajima T, Nenoi M. Chronic restraint-induced stress has little modifying effect on radiation hematopoietic toxicity in mice. J. Radiat. Res. 2015; 56: 760-767.

[23] Lu DY, Li Y, Bi ZW, Yu HM, Li XJ. Aquaporin 1 expression in the testis, epididymis and vas deferens of postnatal ICR mice. Cell Biol. Int. 2008; 32: 532-541.

[24] Zhang S, Niu Q, Gao H, Ma R. Excessive apoptosis and defective autophagy contribute to developmental testicular toxicity induced by fluoride. Environ. Pollut. 2016; 212: 97-104.

[25] Li H, Zhang H, Xie Y, He Y, Miao G, Yang L, Di C, He Y. Proteomic analysis for testis of mice exposed to carbon ion radiation. Mutat. Res. 2013; 755: 148-155.

[26] Saiki S, Sasazawa Y, Imamichi Y, Kawajiri S, Fujimaki T, Tanida I, Kobayashi H, Sato F, Sato S, Ishikawa K, Imoto M, Hattori N. Caffeine induces apoptosis by enhancement of autophagy via PI3K/Akt/mTOR/p70S6K inhibition. Autophagy. 2011; 7: 176-187.

[27] Gu YH, Wang Y, Bai Y, Liu M, Wang HL. Endoplasmic reticulum stress and apoptosis via PERK-eIF2α-CHOP signaling in the methamphetamine-induced chronic pulmonary injury. Environ, Toxicol. Pharmacol. 2017; 49: 194-201.

[28] Hu BS, Tan JW, Zhu GH, Wang DF, Zhou X, Sun ZQ. WWOX induces apoptosis and inhibits proliferation of human hepatoma cell line SMMC-7721.World J. Gastroenterol. 2012; 18: 3020-3026.

[29] Fan C, Zheng W, Fu X, Li X, Wong YS, Chen T. Enhancement of auranofin-induced lung cancer cell apoptosis by selenocystine, a natural inhibitor of TrxR1 in vitro and in vivo. Cell Death Dis. 2014; 5: e1191.

[30] Sou SN, Ilieva KM, Polizzi KM. Binding of human BiP to the ER Stress Transducers IRE1 and PERK Requires ATP. Biochem. Biophys, Res. Commun. 2012; 420: 473-478.

[31] Oyadomari S. Roles of CHOP/GADD153 in endoplasmic reticulum stress. Cell. Death. Differ. 2004; 11: 381-389.

[32] Cao J, Dai DL, Yao L, Yu HH, Ning B, Zhang Q, Chen J, Cheng WH, Shen W, Yang ZX. Saturated fatty acid induction of endoplasmic reticulum stress and apoptosis in human liver cells via the PERK/ATF4/CHOP signaling pathway. Mol. Cell. Biochem. 2012; 364: 115-129.

[33] Liu X, Wang M, Chen H, Guo Y, Ma F, Shi F, Bi Y, Li Y. Hypothermia Protects the Brain from transient global ischemia/reperfusion by attenuating endoplasmic reticulum response-induced apoptosis through CHOP. PLoS One. 2013; 8: e53431.

[34] Quan C, Wang C, Duan P, Huang W, Chen W, Tang S, Yang K. Bisphenol A induces autophagy and apoptosis concurrently involving the Akt/mTOR pathway in testes of pubertal SD rats. Environ. Toxicol. 2017; 32: 1977-1989.

[35] Kang R, Zeh HJ, Lotze MT, Tang D. The Beclin 1 network regulates autophagy and apoptosis. Cell. Death. Differ. 2011; 18: 571-580.

[36] Xue LX, Xu ZH, Wang JQ, Cui Y, Liu HY, Liang WZ, Ji QY, He JT, Shao YK, Mang J, Xu ZX. Activin A/Smads signaling pathway negatively regulates oxygen glucose deprivation-induced autophagy via suppression of JNK and p38 MAPK pathways in neuronal PC12 cells. Biochem. Biophys. Res. Commun. 2016; 480: 355-361.

[37] Pyo JO, Yoo SM, Ahn HH, Nah JS, Hong H, Kam TI, Jung S, Jung YK. Overexpression of Atg5 in mice activates autophagy and extends lifespan. Nat. Commun. 2013; 4: 2300.

[38] Komatsu M, Kageyama S, Ichimura Y. p62/SQSTM1/A170: physiology and pathology. Pharmacol. Res. 2012; 66: 457-462.

[39] Heras-Sandoval D, Pérez-Rojas JM, Hernández-Damián J, Pedraza-Chaverri J. The role of PI3K/AKT/mTOR pathway in the modulation of autophagy and the clearance of protein aggregates in neurodegeneration. Cell Signal. 2014; 26: 2694-2701.

[40] Xu S, Ge J, Zhang Z, Zhou W. MiR-129 inhibits cell proliferation and metastasis by targeting ETS1 via PI3K/AKT/mTOR pathway in prostate cancer. Biomed Pharmacother. 2017; 96:634-641.

[41] Kim AD, Kang KA, Kim HS, Kim DH, Choi YH, Lee SJ, Kim HS, Hyun JW. Ginseng metabolite, compound K, induces autophagy and apoptosis via generation of reactive oxygen species and activation of JNK in human colon cancer cells. Cell Death Dis. 2013; 4: e750.

[42] Feng Z, Liu L, Zhang C, Zheng T, Wang J, Lin M, Zhao Y, Wang X, Levine AJ, Hu W. Chronic restraint stress attenuates p53 function and promotes tumorigenesis. Proc. Natl. Acad. Sci. 2012; 109: 7013-7018.

[43] Lee E, Wei Y, Zou Z, Tucker K, Rakheja D, Levine B, Amatruda JF. Genetic inhibition of autophagy promotes p53 loss-of-heterozygosity and tumorigenesis. Oncotarget. 2016; 7 (42): 67919-67933.

[44] Brentnall M, Rodriguez-Menocal L, De Guevara RL, Cepero E, Boise LH. Caspase-9, caspase-3 and caspase-7 have distinct roles during intrinsic apoptosis. BMC. Cell. Biol. 2013; 14: 32.

[45] Liu D, Zhang H, Gu W, Liu Y, Zhang M. Neuroprotective effects of ginsenoside Rb1 on high glucose-induced neurotoxicity in primary cultured rat hippocampal neurons. PLoS One. 2013; 8 (11): e79399.

[46] Adams JM, Cory S. Bcl-2-regulated apoptosis: mechanism and therapeutic potential. Curr. Opin. Immunol. 2007; 19 (5): 488-496.

[47] Lin CC, Kuo CL, Lee MH, Lai KC, Lin JP, Yang JS, Yu CS, Lu CC, Chiang JH, Chueh FS, Chung JG. Wogonin triggers apoptosis in human osteosarcoma U-2 OS cells through the endoplasmicreticulum stress, mitochondrial dysfunction and caspase-3-dependent signaling pathways. Int. J. Oncol. 2011; 39: 217-224.

[48] Kapuy O, Vinod PK, Bánhegyi G. mTOR inhibition increases cell viability via autophagy induction during endoplasmic reticulum stress - An experimental and modeling study. FEBS Open Bio. 2014; 4: 704-713.